J Biomol NMR (2010) 48:157–167
DOI 10.1007/s10858-010-9446-4

ARTICLE

Signal enhancement in protein NMR using the spin-noise tuning optimum

Martin Nausner · Michael Goger · Eli Bendet-Taicher · Judith Schlagnitweit · Alexej Jerschow · Norbert Müller

Received: 2 July 2010 / Accepted: 27 August 2010 / Published online: 6 October 2010

Abstract We have assessed the potential of an alternative probe tuning strategy based on the spin-noise response for application in common high-resolution multi-dimensional biomolecular NMR experiments with water signal suppression on aqueous and salty samples. The method requires the adjustment of the optimal tuning condition, which may be offset by several 100 kHz from the conventional tuning settings using the noise response of the water protons as an indicator. Although the radio frequency-pulse durations are typically longer under such conditions, signal-to-noise gains of up to 22% were achieved. At salt concentrations up to 100 mM a substantial sensitivity gain was observed.

Keywords Probe tuning · Spin-noise · Absorbed circuit noise · SNTO · Signal-to-noise gain · Sensitivity

This work was presented first at the joint EUROMAR 2010 and 17th ISMAR Conference (July 4–9, 2010, Florence Italy) supported by the European Science Foundation (ESF) as part of the EMAR programme.

M. Nausner · J. Schlagnitweit · N. Müller (✉)
Institute of Organic Chemistry, Johannes Kepler University, Altenbergerstraße 69, 4040 Linz, Austria
e-mail: norbert.mueller@jku.at
URL: http://www.jku.at/orc/

M. Goger
New York Structural Biology Center, 89 Convent Avenue, New York, NY 10027-7556, USA

M. Nausner · E. Bendet-Taicher · A. Jerschow (✉)
Chemistry Department, New York University, New York, NY 10003, USA
e-mail: Alexej.jerschow@nyu.edu
URL: http://www.nyu.edu/projects/jerschow

Abbreviations

SNTO	Spin-noise tuning optimum
WO	Wobble optimum

Introduction

Bloch predicted in 1946 that nuclear magnetic spin-noise should manifest itself as a weak residual signal from statistically incomplete cancellation of magnetic fluctuations. Later Sleator et al. (1985, 1987) observed this phenomenon at liquid helium temperature. McCoy and Ernst (1989) and independently Guéron and Leroy (1989) demonstrated that spin-noise was observable at ambient sample temperature. Later Crooker et al. (2004) detected spin-noise optically using a technique based on Faraday rotation. Müller and Jerschow (2006) reconstructed a two-dimensional image of the cross section of a phantom consisting of capillary tubes in a standard NMR sample tube exploiting nuclear spin-noise in the presence of magnetic field gradients along different directions without the use of radio-frequency irradiation.

The phenomenon is easily observable today using modern cryogenically cooled probes for a large number ($\sim 10^{20}$–10^{22}) of proton spins (Kocacs et al. 2005; Darrasse and Ginfri 2003) and even with room temperature high resolution probes albeit at somewhat longer accumulation times.

Using hyperpolarization techniques noise detection of NMR spectra of ^{129}Xe solutions (Desvaux et al. 2009) and of ^{1}H liquid water samples (Giraudeau et al. 2010) could be enhanced by orders of magnitude. However, it now appears that these hyperpolarization-enhanced noise detection experiments are rather due to absorbed circuit noise than to spin-noise (Giraudeau et al. 2010).

In experiments using cryogenically cooled probes the contribution of absorbed circuit noise signals is reduced as compared to ambient temperature probes (Giraudeau et al. 2010). Still the weakness of the spin-noise signal raises the question, whether there is a potential for spectroscopic or imaging routine applications, beyond addressing fundamental physical questions.

Recently it was shown that spin-noise can serve as a sensitive indicator of probe tuning under receiving conditions (Marion and Desvaux 2008; Nausner et al. 2009). We have reported an increase of the signal-to-noise ratio of up to 50% in a standard ^{1}H 1D NMR sensitivity test. In the current report we employ this alternative tuning approach using the noise response of water protons as an indicator to test whether these sensitivity gains can be realized under typical conditions of modern multi-nuclear, multi-dimensional bio-molecular NMR, where high sensitivity is a key requirement for efficient experimental performance.

McCoy and Ernst (1989), introduced a description of the behavior of the spin-noise signal based on modified Nyquist (1928) noise equations. Due to the interaction between magnetic spin fluctuations in the sample and electron current fluctuations in the radio-frequency coil, the tuning of the probe affects the spin-noise signal. The total spin-noise power $W(\omega)$ is expressed as a function of the absorptive $a(\Delta\omega)$ and dispersive $d(\Delta\omega)$ components of the NMR signal,

$$W(\omega) = q\frac{1 + a(\Delta\omega)\lambda_r^0}{[1 + a(\Delta\omega)\lambda_r]^2 + [d(\Delta\omega)\lambda_r + 2Q\Delta\omega_c/\omega_c]^2} \quad (1)$$

where $\Delta\omega$ is the resonance offset, $\Delta\omega_c$ is the offset from the rf-circuit's tuning optimum ω_c, and q is a frequency independent factor depending on the circuit resistance and temperature, Q is the circuit's quality factor, and

$$\lambda_r = 1/T_r = \frac{1}{2}\eta Q\gamma\mu_0 M_Z \quad (2)$$

is the radiation damping rate (Mao and Ye 1997), with the radiation damping time T_r, the longitudinal magnetization M_z, the filling factor η, and the permeability of free space μ_0. Any disparity between the sample temperature T_s and the circuit temperature T_c is taken into account by the parameter

$$\lambda_r^0 = \lambda_r\frac{T_s}{T_c} = \lambda_r\vartheta \quad (3)$$

For probes, where the sample and the receiver coil are held at the same temperature $\vartheta = 1$, while for cryogenically cooled high resolution NMR probes $\vartheta \gg 1$, i.e. with current technology commonly $\vartheta > 10$.

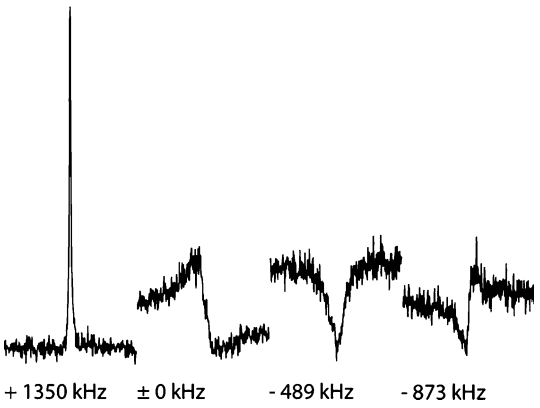

Fig. 1 ^{1}H spin-noise signals of water at different tuning offsets on a 500 MHz spectrometer (Bruker DRX) with ^{1}H/^{13}C/^{15}N triple resonance cryogenically cooled probe (Bruker TXI). The "dip" line shape characteristic of optimum tuning conditions was found at a tuning offset of −489 kHz. Note that the baseline corresponds to the total noise power level and is not zero

The line-shape of the spin-noise power signal may yield either a positive signal ("bump") or a negative signal ("dip") relative to the thermal noise level or various mixed line-shapes with absorptive and dispersive contributions as exemplified in Fig. 1.

It should be noted explicitly, that the apparent baseline in these noise spectra does not represent zero amplitude, but the thermal noise power level of the spectrometer's entire probe and electronic circuitry. The lower the latter, the easier is the observation of spin-noise, making the advancement of cryoprobe technology critical for these studies. The quantum origins of the spin-noise phenomenon have been discussed thoroughly by Hoult and Ginsberg (2001).

For practical purposes, the Nyquist treatment (McCoy and Ernst 1989; Guéron and Leroy 1989; Sleator et al. 1985, 1987; Guéron 1991; Hoult and Ginsberg 2001) provides an adequate account of the line shape changes, but it is difficult to draw quantitative conclusions, in particular about the tuning dependence and frequency shifts of the spin-noise line shape (Nausner et al. 2009). These deviations are likely due to the assumption of an ideal resonance circuit in the derivation of this approach, and could presumably be fixed by a more refined circuit model.

Below we outline practical experimental aspects of achieving sensitivity enhancement by spin-noise aided tuning as they relate to multidimensional biomolecular NMR spectroscopy. As a result, we were able to achieve sensitivity enhancements of 7–22% in HNCO, HNCA, CBCACONH experiments, with no added salt, leading to potential time savings of up to ca. 49%. These demonstration experiments underscore the potential value of applying alternative tuning conditions on high-performance probes in biomolecular NMR.

Materials and methods

Recording spin-noise NMR spectra

On cryogenically cooled probes, the cold pre-amplifiers and cross-diodes are usually directly attached to the probe assembly and cannot be disconnected without major impediment to the probe performance. To minimize the impact of electronic noise generated by the pulse amplifier and other spectrometer hardware, we turn off the mains power supplied to the pulse amplifier (if this is possible without disrupting spectrometer operation, e.g. on Bruker DRX, Avance I and Avance II systems by operating the manual power switch on the proton pulse amplifier) and disconnect the rf-input cable from the cold ^{1}H-pre-amplifier. On standard ambient-temperature-coil probes the procedure is analogous. Some very recent instrument designs (Bruker Avance III) do not allow deactivating the pulse amplifiers completely due to interlinked digital control hardware. In such cases the pulse output cable should be connected to an appropriate dummy load matched in impedance (typically 50 Ω) and power rating to the pulse amplifier used to prevent it from being damaged by accidentally activating pulsing. We wish to emphasize that powering down the amplifier may not be necessary on all spectrometers, but is advisable as a precautionary step in order to not bias the noise measurements.

For the purpose of tuning, spin-noise data are collected using a pseudo 2D acquisition sequence collecting one block of noise per row, usually at a spectral width of ca. 10 ppm with the carrier set off resonance from the water peak (usually 5.5 ppm). Typically a total of 512–1,024 blocks (for samples with high solvent proton concentration, such as proteins in aqueous buffer solution) are collected in this way. Each block (row of the pseudo two-dimensional experiment) is Fourier transformed individually to a complex-valued (phase sensitive) spectrum, which is converted to a power spectrum (accumulating the phase sensitive data would lead to cancellation of the noise signal) e.g.: by using the TopSpin-command xf2 with parameter mc2=ps (Bruker spectrometer software TopSpin versions 1.3 and 2.1). Finally, the rows are summed up (e.g.: TopSpin command f2sum) to yield the one-dimensional noise spectrum.

Continuous acquisition of a noise stream would be more efficient, but is currently impractical to implement due to restrictions in the design of commercial spectrometers. When studying the noise signal line shapes of highly concentrated samples such as solvents, the described method is sufficient and is implemented quite easily.

Finding the spin-noise tuning optimum (SNTO)

For proton-detected experiments on biomolecular samples using H_2O as the main solvent it is most convenient to adjust the SNTO on the ^{1}H noise response of the solvent. Since the heteronuclear channels are not used for receiving, they are tuned in the conventional way.

According to theory (McCoy and Ernst 1989) and as discussed above, a symmetrical "dip" would be observed at the rf-circuit's resonance frequency (i.e. $\Delta\omega_c = 0$). In practice this line-shape may be observed at considerable tuning offsets $\Delta\omega_c$ from the optimum determined by "wobbling". In one example case (Fig. 1) the ^{1}H noise "dip" signal of a water sample was found at $\Delta\omega_c = -489$ kHz. We clarify here that this "dip" inherently originates from absorbed circuit noise, but it is less deep in the presence of spin-noise, which always contributes additional noise power. The tuning offset at which we observe optimum tuning conditions for the receiving circuits, hence called spin-noise tuning optimum (SNTO), varies considerably between different probes. As has been shown recently (Marion and Desvaux 2008; Nausner et al. 2009) acquiring pulsed NMR-spectra under SNTO conditions may enhance the received NMR signal and thus increase the signal-to-noise ratio, although the nominal rf-pulse durations increase.

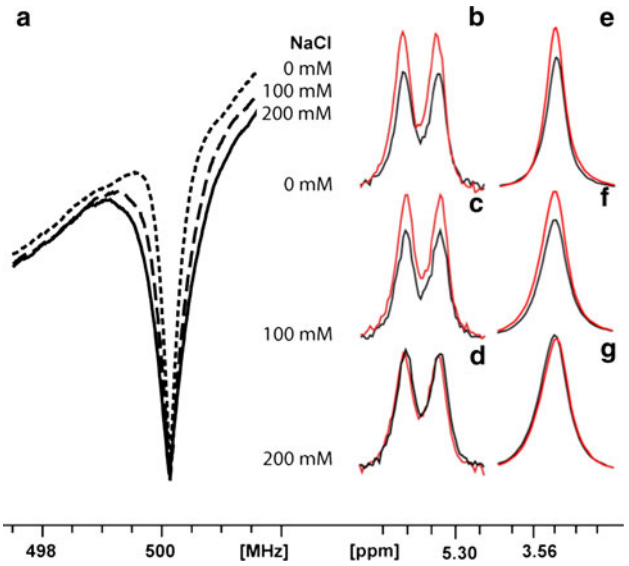

Fig. 2 Tuning ("wobble") curves at different salt concentrations 0 mM (*dotted line*), 100 mM (*dashed line*), 200 mM (*solid line*) (*a*). The anomeric doublet in phase sensitive (absorptive) pulsed ^{1}H NMR spectra of sucrose with 0 mM NaCl (*b*), 100 mM NaCl (*c*), 200 mM NaCl (*d*), and the singlet at 3.56 ppm (with different vertical scaling) with 0 mM NaCl (*e*), 100 mM NaCl (*f*), 200 mM NaCl (*g*) acquired under the following conditions: pre-saturation of the water signal for 1.5 s with an rf-power of $B_1\gamma/(2\pi) \sim 465$ Hz. For both tuning settings the 90° pulse width was separately calibrated and the solvent pre-saturation frequency adjusted for minimum response. A 30° pulse was used in the signal-to-noise tests to allow reduction of the receiver gain above the value required for receiver gain independent sensitivity. The position of the tuning optimum (as determined by Bruker's "wobb" routine) is at zero offset frequency (*solid black line*), while the SNTO is at an offset of –470 ± 40 kHz (*solid red line*)

It is convenient that the observed gain is not constrained to a narrow range around the SNTO offset, but as was demonstrated earlier (Nausner et al. 2009), may provide sensitivity gain over a wider tuning range around the spin-noise "dip" indicator. As a consequence, once the tuning condition is determined in this way, it will be applicable for samples with different solvents as well.

We recommend the following steps when determining the SNTO for the first time on a high resolution, cryogenically cooled probe (We note that different procedures may be required for solids probes as reported by Schlagnitweit et al. 2010): Acquire a noise spectrum of the water signal under conventional tuning conditions first. The noise power signal line shape will usually be asymmetric, resembling a mixed phase peak. The peak asymmetry indicates, in which direction the tuning frequency has to be shifted, to achieve the pure symmetric "dip" line shape. For example, the noise signal shown in Fig. 1 at $\Delta\omega_c = 0$ has its negative wing toward lower tuning frequencies. This is the direction in which the SNTO, i.e. the "dip" line shape will be found. The tuning is then systematically varied (we recommend ca. 200 kHz steps initially) to locate the "dip" position. Matching is adjusted to give the lowest minimum reading of the conventional tuning curve before each measurement. This procedure is repeated until a pure "dip" line shape of the noise signal is found. For different probes (especially non cryogenically cooled ones) other procedures might be required as exemplified by Schlagnitweit et al. 2010 for MAS probes. In that paper it is also found that the tuning situation may be significantly influenced by the particular probe/amplifier combination.

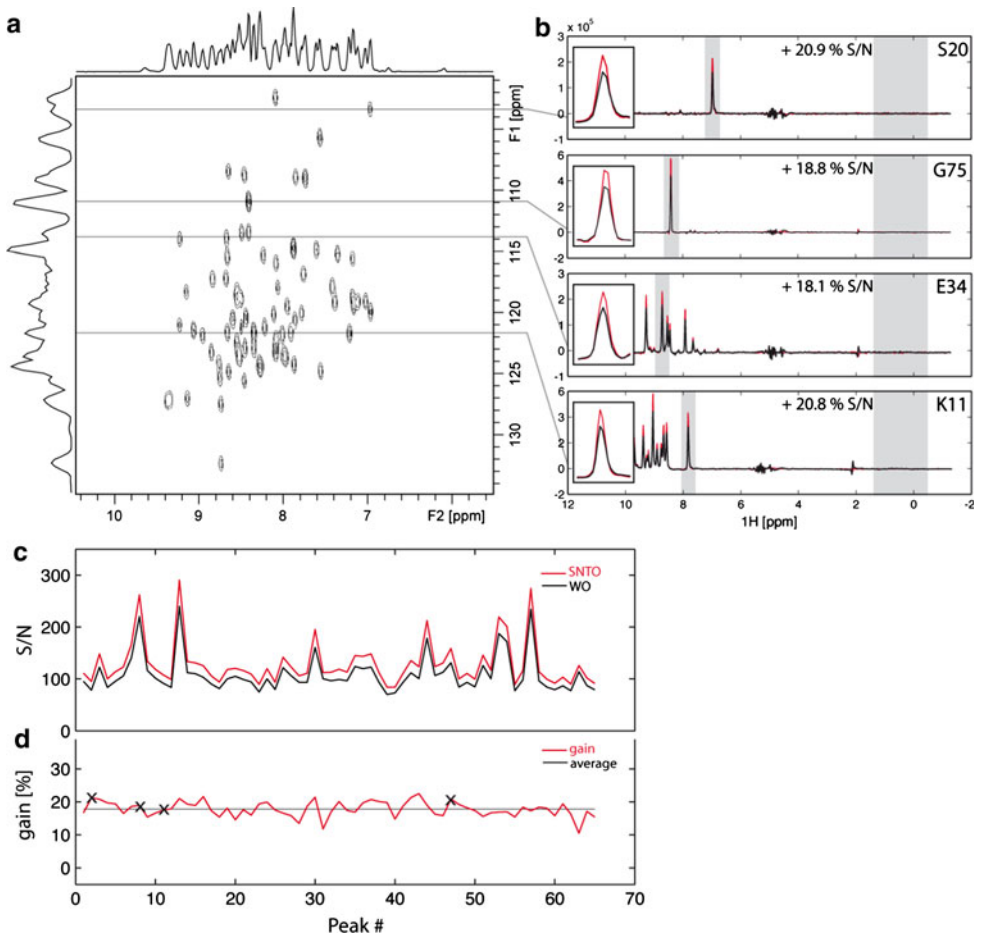

Fig. 3 First [^{1}H ^{15}N] plane of a HNCO spectrum acquired on a 500 MHz spectrometer with a cryogenically cooled triple resonance probe (**a**). For processing the data and evaluating the sensitivity enhancement two different approaches were used. The RMS noise in both cases was determined over the whole ^{15}N shift range in a ^{1}H shift range from −0.5 to 1.5 ppm. For the 1D traces signal-to-noise ratios were calculated in Matlab from amplitudes of selected signals under SNTO conditions (in *red*) and conventional tuning conditions (in *black*), signal ranges and noise ranges used are indicated by *gray blocks* (**b**). In the second approach peak lists were generated with the TopSpin peak picking routine and the signal-to-noise ratios were determined from the listed signal amplitudes. The signal-to-noise ratios for the peak list are plotted for SNTO conditions (in *red*) and conventional tuning conditions (in *black*) (**c**). The resulting gain under SNTO conditions is plotted (in **red**) versus the peak number. The *black horizontal line* indicates the average signal enhancement of 17.8% (**d**). The signals selected in (**b**) are marked with *black crosses* in (**d**)

Data acquisition

The experiments investigating salt effects on the tuning dependence of the SNTO were performed on 2 mM sucrose in 9/1 H_2O/D_2O at salt concentrations of 0, 100, and 200 mM NaCl, both at the SNTO and for comparison at the conventional tuning ("wobble") optimum (WO) (NB: On newer Varian systems, the command corresponding to "wobble" is "mtune").

The spectra presented in Fig. 2 were obtained on a Bruker DRX 500 MHz spectrometer (11.7 T) equipped with a 5 mm high resolution triple resonance (TXI, H, C, N) cryogenically cooled probe (sample temperature 298.3 K, rf-coil temperature 30.5 K). The receiver gain setting was 128, which exceeds the limit above which the *S/N* ratio is independent of this gain setting. This limit was determined in separate experiments, and marks the region above which digitization noise becomes negligible. The parameters used on this particular spectrometer were not the ones recommended for the spectrometer's specification test since the predominant effects of radiation damping made solvent signal suppression extremely irreproducible (even in sequential experiments) and caused varying baseline artifacts, which the built-in ('sino') signal-to-noise calculation routine of TopSpin could not compensate. For this reason we used Matlab to calculate the *S/N* on the real data of the spectrum. In addition we evaluated the *S/N*-performance of the signal at 3.56 ppm, which is not noticeably affected by the solvent signal "wings", and where the *S/N*-values calculated Matlab and TopSpin are virtually identical.

All protein experiments were performed on doubly labeled (^{15}N and ^{13}C) ubiquitin (500 μM) in 50 mM ammonium acetate buffer, pH 4.5, no added salt, both at the SNTO and at the WO for comparison (a sample temperature of 302.2 K, rf-coil temperature 30.5 K). The displayed spectra (Figs. 3, 4, 5, 6) were acquired on a Bruker Avance spectrometer at 500 MHz equipped with cryogenically cooled triple resonance probe optimized for proton detection (TXI) using conditions detailed in Table 1. The 3D pulse sequences used [original HNCO and HNCA sequence by Kay et al. 1990, original CBCA(CO)NH sequence by Grzesiek and Bax 1992a, actual HNCA and HNCO sequence (hncagpwg3d, hncogpwg3d from the Bruker library) by Grzesiek and Bax (1992b), Schleucher et al. (1993), Kay et al. (1994), and Davis et al. (1992), actual CBCA(CO)NH

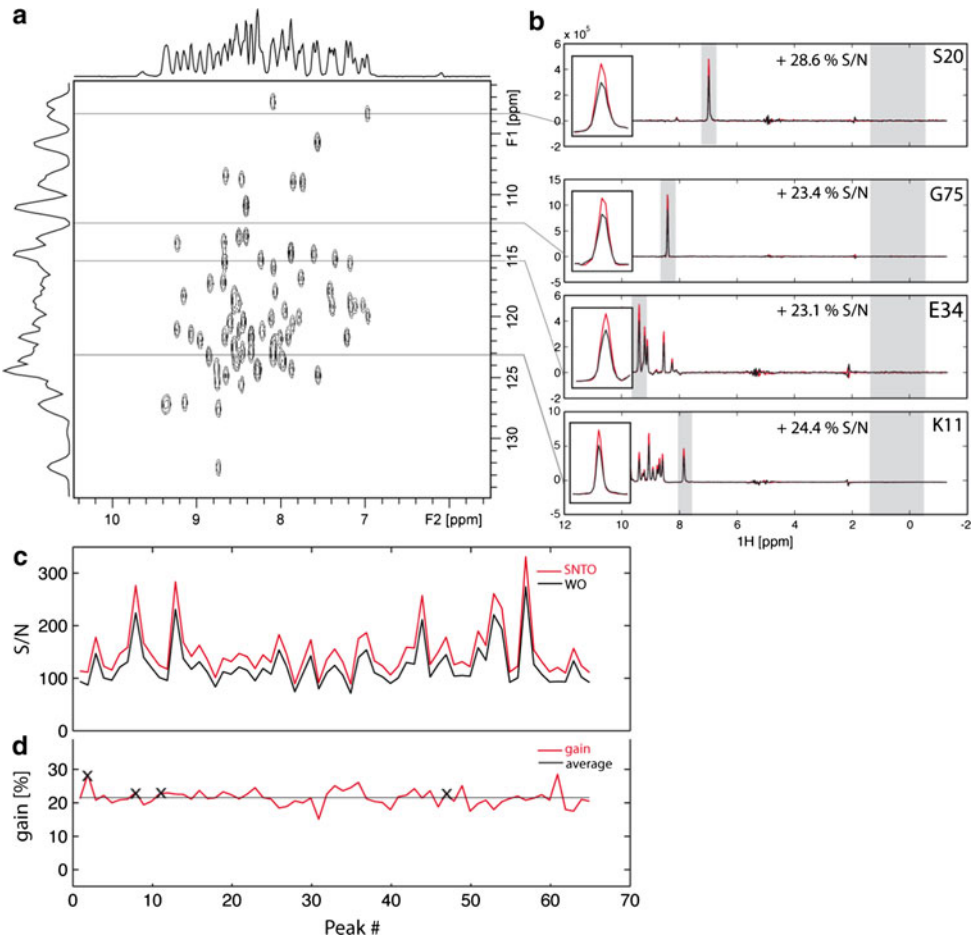

Fig. 4 First [^1H ^{15}N] plane of a HNCA spectrum acquired on a 500 MHz spectrometer with a cryogenically cooled triple resonance probe (**a**). In analogy to Fig. 3b 1D traces of selected signals and *S/N* ratios are displayed under SNTO (in *red*) and WO conditions (*black*) (**b**). In analogy to Fig. 3c and d *S/N* of the TopSpin peak lists are displayed under SNTO (in *red*) and WO conditions (*black*) (**c**), with the resulting *S/N* gain and the average signal enhancement of 21.8% under SNTO conditions (**d**)

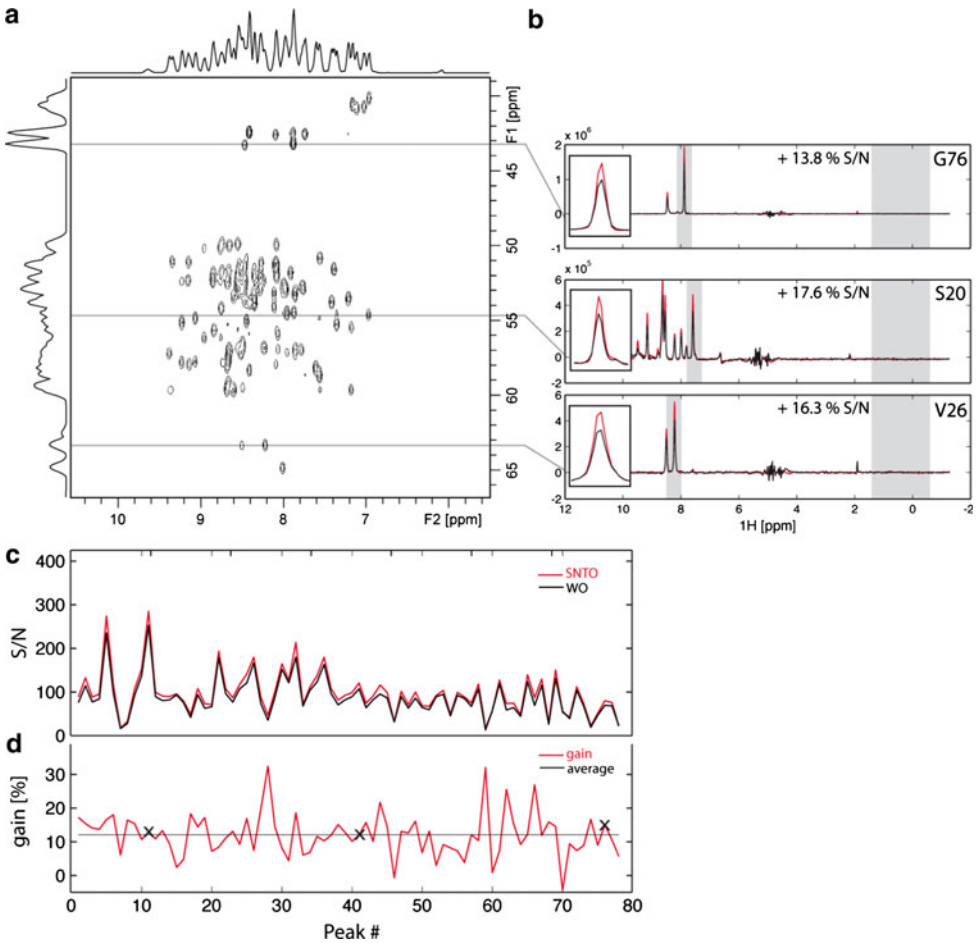

Fig. 5 First [^{1}H ^{13}C] plane of a HNCA spectrum acquired on a 500 MHz spectrometer with a cryogenically cooled triple resonance probe (**a**). In analogy to Fig. 3b 1D traces of selected signals and *S*/*N* ratios are displayed under SNTO (in *red*) and WO conditions (*black*) (**b**). In analogy to Fig. 3c and d *S*/*N* of the TopSpin peak lists are displayed under SNTO (in *red*) and WO conditions (*black*) (**c**), with the resulting *S*/*N* gain and the average signal enhancement of 11.9% under SNTO conditions (**d**)

sequence (cbcaconhgpwg3d from the Bruker library) by Grzesiek and Bax (1993), and Muhandiram and Kay (1994)] used WATERGATE (Sklenar et al. 1993) solvent signal suppression. In all 3D experiments the receiver gain was set to 1,024, which is far above the digitization noise limit.

Data analysis

For evaluating the sensitivity enhancement, two different approaches were used. In both cases the (thermal and electronic) RMS noise levels (*N*), of all 2D planes from 3D spectra were calculated as the average of the root mean square noise of all rows (over the whole ^{15}N/^{13}C shift range) in a ^{1}H shift range from −0.5 to 1.5 ppm.

In the first approach we selected three to four well-isolated signals representatively distributed over the spectral range of interest for analysis of the relative sensitivity. Care was taken that the chosen signals originate from amino acids well spread over the sequence of ubiquitin.

After phasing and fifth order polynomial baseline correction (using Bruker's TopSpin software), the respective rows of the 2D spectral plane (of the multidimensional experiments) were transferred into the Matlab environment to determine the signal amplitudes (*S*) and the noise levels (*N*), as described above, using in-house written Matlab scripts. The signal-to-noise ratio (*S*/*N*) was calculated as *S*/(2**N*). The calculated values are listed in Table 3.

In the second approach peak lists were generated by the TopSpin peak picking routine and the listed signal amplitudes (*S*) were used to determine signal-to-noise ratios for the entire peak list in the same way.

Results and discussion

Parameters influencing the SNTO

Although our previous experiments showed that the position of the SNTO was mainly determined by the probe design (Nausner et al. 2009), there are several parameters that may further influence the position of the SNTO in typical biomolecular NMR samples. The determination of the SNTO requires a reasonably good shim, as inhomogeneous broadening caused by magnetic field gradients quenches radiation damping (see Eqs. 1, 2) and obscures the "dip" line shape (Nausner et al. 2009). In such cases, for ambient temperature

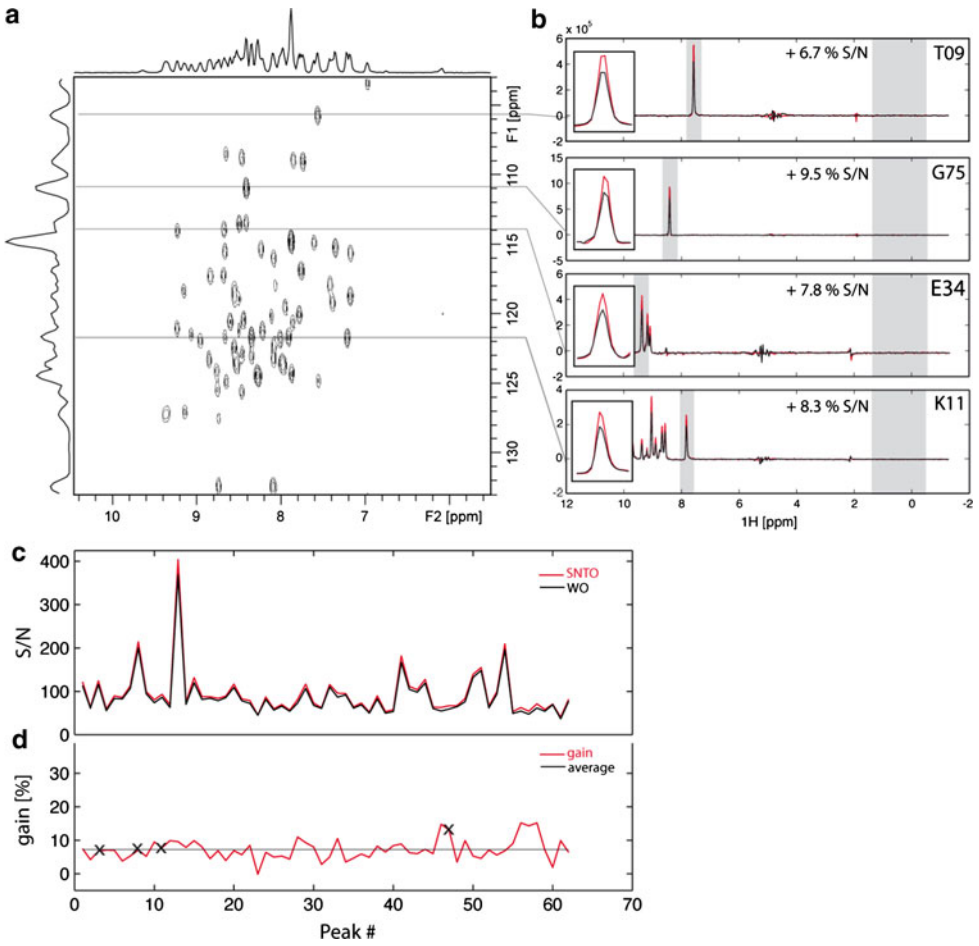

Fig. 6 First [^{1}H ^{15}N] plane of a CBCA(CO)NH spectrum acquired on a 500 MHz spectrometer with a cryogenically cooled triple resonance probe (**a**). In analogy to Fig. 3b 1D traces of selected signals and *S/N* ratios are displayed under SNTO (in *red*) and WO conditions (*black*) (**b**). In analogy to Fig. 3c and d *S/N* of the TopSpin peak lists are displayed under SNTO (in *red*) and WO conditions (*black*) (**c**), with the resulting *S/N* gain and the average signal enhancement of 7.2% under SNTO conditions (**d**)

probes, the NMR noise signals may appear too weak to be observed. For cryogenically cooled probes the observation of a positive "bump" or a complex mixed absorptive/dispersive line shape may occur, depending on the total magnetization and inhomogeneous broadening, thus making the detection of the optimum tuning conditions difficult. A similar behavior has been observed for homogeneous broadening in the presence of paramagnetic substances in the sample. For a detailed discussion of non-linearity and frequency shifts of nuclear magnetic spin-noise we refer to our earlier work (Nausner et al. 2009).

Experiments over the temperature range of typical biomolecular samples, such as proteins and nucleic acids, i.e. 5–50°C revealed no measurable effects of sample temperature on the SNTO. In this investigation we use buffered aqueous samples, which represent typical media for NMR studies of biomolecules. Ionic strengths and conductivities of such solutions are known to be major factors influencing probe tuning, matching and pulse performance (Kelly et al. 2002; Horiuchi et al. 2005; Gadian and Robinson 1979; Hoult 1996). Salt concentrations of 200 mM in biological samples are known to decrease the sensitivity significantly, especially when using cryogenically cooled probes.

It was hence suspected that the signal enhancement reported at the spin-noise tuning optimum would change with salt concentration as well.

Figure 2a illustrates how the minimum of the tuned and matched "wobble" curve broadens (i.e. loss of sensitivity) with increasing salt concentration.

Figure 2 shows the anomeric doublet (b–d) of sucrose, as well as the singlet signal at 3.56 ppm (e–g) obtained under conventional tuning conditions (black lines), and under SNTO conditions (red lines).

With no salt in the sample, a signal-to-noise gain of about 25% is easily achievable via SNTO optimization. Even after addition of 100 mM NaCl a signal-to-noise gain of about 20% is provided by this tuning method. For 200 mM NaCl, probe tuning becomes relatively insensitive and hardly any effect on signal-to-noise intensity is observable. In addition the SNTO frequency was shifted by about 100 kHz further away from the transmission optimum.

Sensitivity enhancement

There is considerable gain in signal-to-noise ratio for all obtained multidimensional spectra under SNTO conditions

Table 1 Acquisition parameters of the multi-dimensional NMR experiments used for the protein test spectra, where $\Delta\omega_c$ is the tuning offset in kHz, Nuc is the nucleus, TD is the number of time domain data points in each FID, SW is the spectral width in ppm, $\omega 0$ is the carrier chemical shift in ppm, PD is the duration of the 90° ^{1}H high power pulse in μs, DD is the pulse duration of the decoupling pulse in μs, PP is the power level of the hard pulse in kHz, and the receiver gain was 1,024 for all spectra

	$\Delta\omega_c$	Nuc	TD	SW	$\omega 0$	PD	PP	DD
hncogpwg3d								
WO	0	^{1}H	1,024	12	4.7	9.45	26.45	60
SNTO	−165	^{1}H	1,024	12	4.7	10.3	24.27	60
		^{15}N	128	35	118		6.41	200
		^{13}C	1	25	176			
hncagpwg3d								
WO	0	^{1}H	1,024	12	4.7	9.45	26.45	60
SNTO	−165	^{1}H	1,024	12	4.7	10.3	24.27	60
		^{15}N	128	35	118		6.41	200
		^{13}C	1	25	176			
WO	0	^{1}H	1,024	12	4.7	9.45	26.45	60
SNTO	−165	^{1}H	1,024	12	4.7	10.3	24.27	60
		^{15}N	1	35	118		6.41	200
		^{13}C	128	32	54			
cbcaconhgp3d								
WO	0	^{1}H	1,024	12	4.7	9.45	26.45	60
SNTO	−165	^{1}H	1,024	12	4.7	10.3	24.27	60
		^{15}N	128	30	118		6.41	200
		^{13}C	1	75	39			

Table 2 Effect of salt concentration on the signal-to-noise ratio and the related signal-to-noise gains at the SNTO of the anomeric doublet of sucrose at 5.29 ppm and the singlet signal at 3.56 ppm

c_{NaCl}	SNTO				WO				Gain
	S	*N*	*S/N*	PD	*S*	*N*	*S/N*	PD	*S/N%*
Signal 5.29 ppm									
0	1.69e+04	220.6	38.2	12.98	1.26e+04	207.5	30.4	8.43	25.7
100	1.56e+04	245.2	31.8	13.25	1.18e+04	227.4	26.0	10.44	22.2
200	1.31e+04	251.5	26.0	14.39	1.28e+04	238.4	26.8	12.08	−2.9
Signal 3.56 ppm									
0	6.69e+04	114.7	291.5	12.98	5.47e+04	109.8	249.0	8.43	14.5
100	5.77e+04	124.6	231.5	13.25	4.65e+04	116.3	200.0	10.44	16.5
200	4.59e+04	128.4	178.6	14.39	4.71e+04	125.4	187.7	12.08	−4.9

The signal at 5.29 ppm was processed without any window function using a 1.5 ppm noise region (between 6 and 9 ppm) giving relatively low signal-to-noise ratios. The signal at 3.56 ppm was processed with an exponential window function with 0.3 Hz line broadening. It is not influenced significantly by the residual wings of the water signal. The difference between the signal-to-noise ratios reported here and typical values reported by instrument manufacturers are presumably due to stronger solvent suppression, which was essential to increase the RG to 128 and to provide reproducible suppression of the water signal over a large tuning range of up to 1 MHz. Results for both signals are listed, c_{NaCl} is the salt concentration in mM, *S* is the signal amplitude, *N* is the RMS noise value of the spectrum, *S/N* is the resulting signal-to-noise ratio, PD is the duration of the 90° ^{1}H high power pulse in μs, *S/N%* is the signal-to-noise gain under SNTO conditions

compared to the WO conditions. The average *S/N* gain for the [^{1}H ^{15}N] HNCO and [^{1}H ^{15}N] HNCA 2D planes of the spectra of ubiquitin with no additional salt is about 18–22%. Detailed data can be found in Figs. 3, 4, 5, and 6 and Table 3.

Upon inspecting the data more closely, there appears to be a trend of decreasing gain from SNTO-tuning with an increasing number of pulses (and duration) of the pulse sequences. At this time, we have no good explanation of this dependence. It is possible, however, that the decrease

Table 3 Signal-to-noise gains of selected signals in 3D protein experiments on ubiquitin

	SNTO			WO			Gain
	S	*N*	*S/N*	*S*	*N*	*S/N*	*S/N%*
HNCO [^{1}H ^{15}N]							
Figure 3							
S20 (Row 118)	2.13e+05	1113.8	95.6	1.60e+05	1013.28	79.1	20.9
T9 (Row 110)	3.31e+05		148.7	2.50e+05		123.3	20.6
G75 (Row 90)	5.85e+05		262.6	4.48e+05		221.1	18.8
E34 (Row 79)	2.35e+05		105.7	1.81e+05		89.5	18.1
K11 (Row 51)	3.55e+05		159.4	2.67e+05		132.0	20.8
A46 (Row 12)	2.04e+05		91.7	1.61e+05		79.6	15.2
HNCA [^{1}H ^{15}N]							
Figure 4							
S20 (Row 118)	4.80e+05	2172.2	110.5	3.49e+05	2030.5	85.9	28.6
T9 (Row 110)	7.68e+05		176.8	5.93e+05		146	21.1
G75 (Row 90)	1.19e+06		275.0	9.05e+05		222.9	23.4
E34 (Row 79)	5.25e+05		120.9	3.99e+05		98.2	23.1
K11 (Row 51)	6.8e+06		156.6	5.11e+05		125.9	24.4
A46 Row 12	4.78e+05		110.0	3.70e+05		91.1	20.8
HNCA [^{1}H ^{13}C]							
Figure 5							
G76 (Row 215)	1.91e+06	3323.8	287.5	1.46e+06	2895.8	252.6	13.8
S20 (Row 123)	5.02e+05		75.5	3.72e+05		64.2	17.6
V26 (Row 54)	5.39e+05		81.1	4.04e+05		69.7	16.3
CBCACONH [^{1}H ^{15}N]							
Figure 6							
T9 (Row 117)	5.49e+05	2200.1	124.7	4.18e+05	1791.0	116.8	6.7
G75 (Row 94)	9.28e+05		210.9	6.90e+05		192.7	9.5
E34 (Row 82)	4.12e+05		93.7	3.11e+05		86.9	7.8
G76 (Row 78)	1.78e+06		404.7	1.32e+06		369.3	9.6
K11 (Row 49)	2.57e+05		58.4	1.93e+05		53.9	8.3

Signal-to-noise ratios of selected amino acid cross peaks in 2D planes (^{1}H,^{15}N or ^{1}H,^{13}C) of 3D experiments (indicated in the left column) are compared under WO and SNTO tuning conditions. *S* is the signal amplitude of the corresponding signal, *N* is the RMS noise value of the spectrum, *S/N* is the resulting signal-to-noise ratio, *S/N%* is the signal-to-noise gain under SNTO conditions

is at least in part due to the combined influences of increased off-resonance effects at lower effective pulse powers and longer total durations of the pulse sequences. Our data (Figs. 3, 4, 5, 6) however do not show a correlation of enhancement with resonance offset and apparently fluctuate randomly over the chemical shift range.

Figures 3a, 4a, 5a, and 6a show representative examples of 2D planes of the 3D spectra used in this investigation. In Figs. 3b, 4b, 5b, and 6b extracted ^{1}H traces containing the signals selected for *S/N* comparison are displayed. The black spectra were obtained under WO tuning conditions, and those in red under SNTO conditions. Gray blocks indicate the regions used for *S/N* calculation. Figures 3c, 4c, 5c, and 6c compare signal-to-noise ratios determined from the signal amplitudes in the peak lists (generated with the TopSpin peak picking routine) and the corresponding sensitivity gains are displayed in Figs. 3d, 4d, 5d, and 6d.

We have performed similar tests on a variety of instruments (data not shown here) but have only used the most completely documented cases for this report. In general, while the position of the SNTO varies significantly, similar behavior and enhancements have been found with different equipment. The actual enhancements observed vary and apparently depend primarily on the particular probe circuits and pre-amplifiers. Matching can also be an important parameter as shown for solid state applications very recently (Schlagnitweit et al. 2010). Usually the enhancement achieved is larger, if the tuning offset is large, but it may fall off rapidly, if the offset approaches the mechanical end of the capacitors' tuning range.

We have also been working recently with some newer cryogenically cooled probes, where apparently the SNTO and the WO nearly coincide, which precludes any benefit from this alternative tuning approach. Actually achieving such a situation may be a worthwhile design goal for high performance probes. (Webb 2006).

An additional matching circuit has been proposed (Marion and Desvaux 2007; Marion and Desvaux 2008). It would allow for separate tuning and matching under pulse and receiving conditions. It cannot easily be retrofitted to existing cryogenically cooled probes, since the preamplifiers are directly attached to the proper probes and enclosed within the cooling manifold.

Conclusion

Tuning high performance NMR probes, in particular cryogenically cooled ones, according to spin-noise tuning optimum conditions (Nausner et al. 2009), may considerably improve the signal-to-noise ratio of multi-dimensional NMR experiments that are commonly used for the investigation of biological macromolecules. Once the SNTO condition is found for a specific setup (probe and preamplifier), and the pulses are calibrated at this new tuning condition, one can benefit from the associated sensitivity enhancement without readjustment for different samples, except at high salt concentrations. The physical rationale behind this behavior is that tuning under receiving (low voltage conditions) is generally different from tuning under pulse conditions and therefore a different response is expected. In particular impedance matching to the preamplifier will be affected by different tuning conditions.

On an ideal probe, in theory, tuning offsets should affect noise and signal in the same way. On the other hand, under real conditions (i.e. with multiply tuned and compromise-matched coils) and with significant noise contributions from sources in the receiving chain between the rf-coil and the digitizer, the total *S/N*-ratio apparently benefits significantly from this noise tuning approach.

Under these conditions, the rf-pulses are typically longer than under transmission tuning conditions (i.e. conventional tuning). Since most biomolecular NMR experiments are performed in aqueous solutions, where there is a dominant water proton signal, spin-noise data for the determination of best reception tuning conditions can be acquired straightforwardly. Although an increase of salt concentration reduces the potential gain, as it noticeably degrades the quality factor of the probe circuit (Fig. 2), almost the full SNTO *S/N* enhancement is still achievable for up to 100 mM NaCl.

Most biomolecular NMR experiments today are performed with ^{1}H detection. For cases of heteronuclear detection (Serber et al. 2000; Bermel et al. 2006) one could use a similar procedure based on a highly isotope-enriched test sample, or make use of maximizing the resonance circuit's intrinsic noise (Marion and Desvaux 2008).

Another possibility would be to determine the *S/N* changes as a function of tuning offset while recalibrating the rf pulses on the nucleus in question.

The tuning offsets and associated signal gains we observed for ^{1}H detected experiments are particular to specific probe-preamplifier combinations, but have been found to be representative of the situations found on a variety of instruments. Determining the optimal tuning conditions under receiving conditions can lead to significant time-savings for biomolecular NMR experiments due to the sensitivity enhancement obtainable with existing hardware.

Acknowledgments This work was supported by the Austrian Marshall Plan Foundation (to Nausner M), the FWF (Austrian Science Funds) Project No. P19635-N17 (to Müller N), a grant (to Jerschow A) by the US NSF (CHE-0550054). We acknowledge inspiring discussions with Bain AD, Bermel W, Desvaux H, Itin B, Otting G, and Sleator T. The NMR facilities of the New York Structural Biology Center were used in this work. These facilities are supported by the New York State Office of Science, Technology, and Academic Research, and the National Institutes of Health (grant P41 FM66354).

References

Bermel W, Bertini I, Felli IC, Piccioli M, Pierattelli R (2006) ^{13}C-detected protonless NMR spectroscopy of proteins in solution. Progr NMR Spectrosc 48:25–45

Bloch F (1946) Nuclear induction. Phys Rev 70:460–475

Crooker SA, Rickel DG, Balatsky AV, Smith DL (2004) Spectroscopy of spontaneous spin noise as a probe of spin dynamics and magnetic resonance. Nature 431:49–52

Darrasse L, Ginfri J-C (2003) Perspectives with cryogenic RF probes in biomedical MRI. Biochimie 85:915–937

Davis AL, Boelens R, Kaptein R (1992) Rapid acquisition of three-dimensional triple-resonance experiments using pulsed field gradient techniques. J Biomol NMR 2:395

Desvaux H, Marion DJ-Y, Huber G, Berthault P (2009) Nuclear spin-noise spectra of hyperpolarized systems. Angew Chem Int Ed 48:4341–4343

Gadian DR, Robinson FNH (1979) Radiofrequency losses in NMR experiments on electrically conducting samples. J Magn Reson 34:449–455

Giraudeau P, Müller N, Jerschow A, Frydman L (2010) ^{1}H NMR noise measurements in hyperpolarized liquid samples. Chem Phys Lett 489:107–112

Grzesiek S, Bax A (1992a) Correlating backbone amide and side chain resonances in larger proteins by multiple relayed triple resonance NMR. J Am Chem Soc 114:6291–6293

Grzesiek S, Bax A (1992b) Improved 3D triple-resonance NMR techniques applied to a 31 kDa protein. J Magn Reson 96:432–440

Grzesiek S, Bax A (1993) Amino acid type determination in the sequential assignment procedure of uniformly $^{13}C/^{15}N$-enriched proteins. J Biomol NMR 3:185–204

Guéron M (1991) A coupled resonator model of the detection of nuclear magnetic resonance, radiation damping, frequency pushing, spin noise, and the signal-to-noise ratio. Magn Reson Med 19:31–41

Guéron M, Leroy JL (1989) NMR of water protons. The detection of their nuclear-spin noise, and a simple determination of absolute probe sensitivity based on radiation damping. J Magn Reson 85:209–215

Horiuchi T, Takahashi M, Kikuchi J, Yokoyama S, Maeda H (2005) Effect of dielectrical properties of solvents on the quality factor for a beyond 900 MHz cryogenic probe model. J Magn Reson 174:34–42

Hoult DI (1996) Sensitivity of the *NMR* experiment. Encycl NMR 7:4256–4266

Hoult DI, Ginsberg NS (2001) The quantum origins of the free induction decay and spin noise. J Magn Reson 148:182–199

Kay LE, Kura M, Tschudin R, Bax A (1990) Three-dimensional triple-resonance NMR spectroscopy of isotopically enriched proteins. J Magn Res 89:496–514

Kay LE, Xu GY, Yamazaki T (1994) Enhanced-sensitivity triple-resonance spectroscopy with minimal H_2O saturation. J Magn Reson A 109:129–133

Kelly AE, Ou HD, Withers R, Dötsch V (2002) Low-conductivity buffers for high-sensitivity NMR measurements. J Am Chem Soc 124:12013–12019

Kocacs H, Moskau D, Spraul M (2005) Cryogenically cooled probes—a leap in NMR technology. Prog Nucl Magn Reson Spectrosc 46:131–155

Mao X-A, Ye C-E (1997) Understanding radiation damping in a simple way. Conc Magn Reson 9:173–187

Marion DJ-Y, Desvaux H (2007) Procédé de réglage d'un circuit d'excitation et de détection pour résonance magnétique nucléaire et circuit d'excitation et de détection adapté à la mise en oeuvre d'un tel procédé. French patent with extensions, Number FRA 0708464, European patent number EP 2 068 164, 4 December 2007. Published June 04 2009

Marion DJ-Y, Desvaux H (2008) An alternative tuning approach to enhance NMR signals. J Magn Reson 193:153–157

McCoy MA, Ernst RR (1989) Nuclear spin noise at room temperature. Chem Phys Lett 159:587–593

Muhandiram DR, Kay LE (1994) Gradient-enhanced triple-resonance three-dimensional NMR experiments with improved sensitivity. J Magn Res B 103:203–216

Müller N, Jerschow A (2006) Nuclear spin noise imaging. Proc Nat Acad Sci USA 103:6790–6792

Nausner M, Schlagnitweit J, Smrecki V, Yang X, Jerschow A, Müller N (2009) Non-linearity and frequency shifts of nuclear magnetic spin-noise. J Magn Reson 198:73–79

Nyquist H (1928) Thermal agitation of electric charge in conductors. Phys Rev 32:110–113

Schlagnitweit J, Dumez J-N, Nausner M, Jerschow A, Elena-Herrmann B, Müller N (2010) Observation of NMR noise from solid samples, J Magn Reson (2010, accepted for publication)

Schleucher J, Sattler M, Griesinger C (1993) Coherence selection by gradients without signal attenuation—application to the 3-dimensional HNCO experiment. Angew Chem Int Ed 32:1489–1491

Serber Z, Richter C, Moskau D, Böhlen JM, Gerfin T, Marek D, Häberli M, Baselgia L, Laukien F, Stern AS, Hoch JC, Dötsch V (2000) New carbon-detected protein NMR experiments using CryoProbes. J Am Chem Soc 122:3554–3555

Sklenar V, Piotto M, Leppik R, Saudek V (1993) Gradient-tailored water suppression for 1H–15N HSQC experiments optimized to retain full sensitivity. J Magn Reson Ser A 102:241–245

Sleator T, Hahn EL, Hilbert C, Clarke J (1985) Nuclear-spin noise. Phys Rev Lett 55:1742–1746

Sleator T, Hahn EL, Hilbert C, Clarke J (1987) Nuclear-spin noise and spontaneous emission. Phys Rev B 36:1969–1981

Webb AG (2006) Advances in probe design for protein NMR. Annu Rep NMR Spectros 58:1–50